Centrifuge modelling of rainfall-induced slope instability in sand and silty sand

Modélisation centrifuge de l'instabilité de pente induite par la pluie dans un sable et un sable silteux

Vasileios Matziaris, Mohsen S. Masoudian, Alec M. Marshall, Charles M. Heron
Nottingham Centre for Geomechanics, The University of Nottingham, United Kingdom

ABSTRACT: Rainfall-induced instability in slopes is an important challenge around the world. This paper aims to provide a better understanding of the processes involved when modelling slopes in a geotechnical centrifuge by presenting data from tests with two types of soil under two rainfall conditions. Results show that slopes with pure sand do not fail under low and high rainfall intensity whereas a slope comprising the same sand but with 10% silt (i.e. a silty sand), failed under both low and high rainfall intensity. In case of the silty sand slope with low rainfall intensity, a failure occurred even though the relative intensity of the rainfall (i.e. ratio of rate of rainfall to saturated permeability of the soil) was lower than that of pure sand with high rainfall intensity. The different results obtained for the two types of soil are explained by the difference in their permeability and the physical phenomena at grain scale.

RÉSUMÉ : L'instabilité induite par les précipitations dans les talus est un défi important à travers le monde. Cet article vise à mieux comprendre les processus associés à ce problème en présentant les données des essais de centrifuge géotechnique avec deux types de sols sous deux conditions pluviométriques différentes. Les résultats montrent que les talus de sable pur ne rompent pas sous une intensité pluviométrique faible ou élevée, alors qu'une pente comprenant le même sable mais avec 10% de limon (c'est-à-dire un sable limoneux) rompt sous une intensité pluviale basse et élevée. Dans le cas de la pente de sable silteux à faible intensité de précipitations, une rupture s'est produite même si l'intensité relative des précipitations (c'est-à-dire le taux de précipitation par rapport à la perméabilité saturée du sol) est inférieure à celle du sable pur avec une intensité pluviométrique élevée. Les différents résultats obtenus pour les deux types de sol ont été expliqués par la différence de leur perméabilité et les phénomènes physiques à l'échelle du grain.

KEYWORDS: physical modelling, slope stability, geotechnical centrifuge, rainfall

1 INTRODUCTION

Occurrences of failures in natural and man-made slopes during or following periods of intense or prolonged rainfall have been reported in the literature (Guzzetti et al., 2008). During rainfall events, the rainwater infiltrates into the soil and changes the patterns of pore pressure and groundwater flow. Studies have attributed the rainfall-induced slope failures to two distinct mechanisms. The first mechanism is the build-up of the positive pore pressure at the toe of the slope or at the weakest plane of the slope (e.g. interface of superficial soil with the bedrock), which can lead to the static liquefaction of soil. The second mechanism is related to the loss of suction within zones of unsaturated soil following rainfall infiltration, hence the saturation-dependent shear strength governs this failure process (Zhang et al., 2011).

Many studies have adopted physical modelling to study rainfall-induced slope instabilities. 1-g physical models (e.g. Tohari et al., 2007) may not properly represent the full-scale problem, mainly due to their lower stress levels. As a result, the failure in 1-g physical models may need an artificial failure mechanism (e.g. external load in Germer and Braun, 2011). On the other hand, centrifuge modelling can replicate the stress level within a small scale slope model under increased gravity (N-g). There are a relatively large number of studies investigating rainfall-induced slope instabilities using a geotechnical centrifuge. Although some of these studies have considered different types of soil with different sand, silt and clay contents, they have not considered the significance of grain size distribution on the coupled poro-mechanical response of the slope. The closest attempt to study the effect of grain size on rainfall-induced slope instabilities is probably the paper by Ling et al. (2009), where slopes made of sand-clay mixtures were subjected to rainfall and post-failure deformations were analysed to estimate the failure threshold for rainfall characteristics, while no monitoring attempt was made on pore water pressure evolution. The pore pressure data is critical for developing links between failure mechanisms and underlying hydro-mechanical processes. The grain-size distribution plays an important role in determining the initial state and intrinsic properties of the slopes and can therefore influence the mechanisms of failure and rainfall infiltration. This paper presents tests which aim to give a better understanding of how grain size affects the hydro-mechanical behaviour of slopes in the centrifuge. In order to achieve this, two soils were used: the first being 100% sand and the second a mixture of the same sand with a small amount (10%) of silt. The results of these tests are presented and the implications of grain size on the stability of slopes are discussed in this paper.

2 TESTING PREPARATION AND PROCEDURE

2 .1 *Centrifuge facility and climatic chamber*

The Nottingham Centre for Geomechanics (NCG) 50g-tonne, 2 m radius geotechnical centrifuge at the University of Nottingham was used for testing the slope models. In order to enable the simulation of slope stability under rainfall and groundwater conditions, Matziaris et al. (2015) constructed a climatic chamber (Figure 1a). The climatic chamber is a plane-strain rigid container with internal dimensions of 700×400×200 mm (Length×Height×Width) made of aluminium with a transparent Perspex window that allows acquisition of digital images of the sub-surface soil within a cross-section across the the plane-strain condition (Length×Height plane). A monochrome CCD camera (Allied Vision Prosilica GC2450) is placed in front of the Perspex window to take images (up to 15 frames per second), used to measure soil deformations using Particle Image Velocimetry (PIV) techniques.

Rainfall is simulated by the flow of water at a pressure of 600 kPa through misting spray nozzles at the end of vertical aluminium hollow rods (Figure 1b) attached to the under-side of the container lid. The droplets had a mean diameter of 30 μm whereas soil surface was covered with a 30 μm woven mesh to prevent erosion. The water for rainfall is supplied from outside the centrifuge through a 4-channel hydraulic slip ring; the flow is controlled and measured using a solenoid valve and

flowmeter, respectively (Figure 1c). The vertical distance from the tip of the nozzles to the surface of the soil was between 70 and 100 mm to minimise the Coriolis effect and the erosion of the soil surface due to droplet impact pressure (Matziaris et al., 2015). The groundwater level is controlled using standpipes that allow drainage of water at specific elevations above the container base. Two water reservoirs made of perforated aluminium plates covered with woven mesh sheets allow the flow of water from inside the container to the standpipes. To monitor the subsurface pore water pressure during testing, two types of miniature pore pressure transducers (PPTs) were used: Druck PDCR-81 transducers and SWT5 tensiometers. These instruments are capable of measuring both positive and negative pore water pressures. The PPTs need to be saturated prior to testing (Take and Bolton, 2003) to ensure readings are able to quickly respond to changes in pore pressure. The PPTs are first subjected to dry air to remove moisture within the porous stones, then a vacuum (-99 kPa) is applied for nearly 30 minutes. De-aired water is then introduced to the PPTs under a pressure of up to 80% of the PPT capacity for at least 24 hours. Different components of the container and the rainfall simulation instruments are depicted in Figure 1; more details on the climatic chamber and instrumentation can be found in Matziaris et al. (2015).

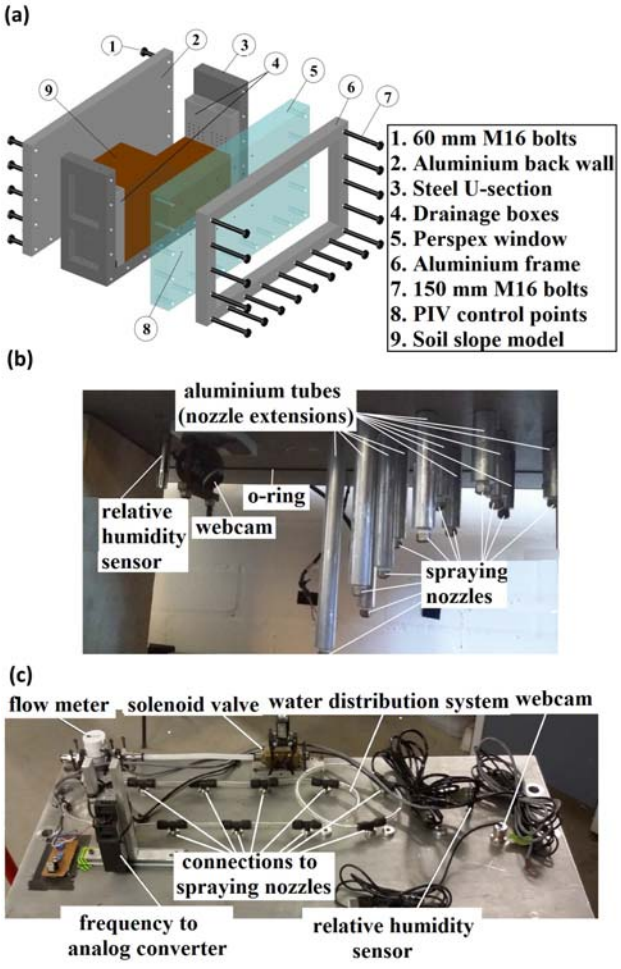

Figure 1. The centrifuge climatic chamber: (a) exploded-view of the plane-strain container (b) spraying nozzles and components inside the box (under container lid) (c) components on top of container lid, including the water distribution system, solenoid valve and flowmeter.

2 .2 *Slope materials and construction*

Two types of soils were used in this study. The sand is a fine silica soil with uniform size distribution (D_{60}/D_{10} = 1.37) and D_{50} of 0.12 mm. In order to construct the slopes, a block of soil was first compacted inside the box and then cut to provide the required geometry. For the sand slope, dry pluviation was adopted; sand was poured from a specific height through a hopper/nozzle calibrated to achieve a relative density of 90±5%. After sand pouring, the soil block was saturated through the drainage valves at the base of the container. The drainage valves were then opened to atmosphere to allow the soil to drain and subsequently a positive air pressure of 20 kPa was applied to facilitate soil desaturation. The created suction within the soil block enabled a slope to be cut at an angle of 50 degrees (higher than the friction angle of 35 degrees), using a sharpened aluminium bar guided by an angle piece fixed to the top of the box. For silty sand, dry soil was first mixed with water at its optimum moisture content and then left in sealed bags to homogenise for 24 hours. The soil was then compacted using a wooden plate and a standard proctor hammer inside the box in 30 mm layers. PPTs were installed at specific locations during model preparation, while a paste of silt was placed at their tips to prevent drying/cavitation before testing. Properties of the soil models tested in this study are given in Table 1.

Table 1. Basic properties of slope models used in centrifuge tests

Slope Parameters	*Sand*	*Silty Sand*
Slope angle (degrees)	50±1	
Slope height (mm)	150	
Total model depth (mm)	250	
Particle density (g/cm^3)	2.62	2.62
Dry density (g/cm^3)	1.5	1.49
Relative density (%)	94	95
Saturated hydraulic conductivity (m/s)	1×10^{-5}	1.2×10^{-6}
Optimum moisture content (%)	11	10.5

2 .3 *Scaling laws*

The scaling factors relevant to the hydro-mechanical processes of this study are provided in Table 2.

2 .4 *Testing Program*

In order to study how different soil materials can influence the results of centrifuge modelling, the two soil types were tested under two different rainfall intensities. Details of these tests are summarised in Table 3, where test IDs are selected so that the first two letters describe the soil type (PS for pure sand and SS for silty sand), and the third letter denotes the rainfall intensity applied (L for low and H for high intensity). All tests were conducted at 60g. The model was brought to 60g in increments of 10g with a pause of approximately 10 minutes at each increment to allow settlement and seepage of excess pore water. Finally, relative intensity refers to the ratio of rainfall rate to the saturated permeability of the soil.

3 RESULTS AND DISCUSSIONS

Introducing rainfall to the model led to development of displacements in all models, due to the infiltration of water within the soil. In tests PS-L and PS-H no failure mechanism was observed, whereas silty sand exhibited failures under both low and high intensities of rainfall (SS-L and SS-H). The rainfall-induced displacements for silty sand tests (SS-L and

SS-H) are presented in Figure 2. The main failure surface starts at the crest of the slope and continues to the mid height of the slope. Theses failures initiated at 1042 hr and 1.25 hr (prototype time) after the rainfall initiation in tests SS-L and SS-H, respectively. Analysis of the time-dependent displacements showed that the failure was sudden for high intensity (SS-H) while a more progressive failure was observed for lower intensity (SS-L).

Table 2. Scaling factors relevant to the current study

Parameter	*Dimension*	*Model*	*Prototype*
Length (macroscopic)	L	1	N
Seepage velocity	L/T	1	1/N
Seepage time (macroscopic)	T	1	N^2
Rainfall duration	T	1	N^2
Rainfall intensity	L/T	1	1/N
Hydraulic gradient (macroscopic)	L/L	1	1/N
Length (grain scale)	L	1	1
Seepage time (grain scale)	T	1	N
Hydraulic gradient (grain scale)	L/L	1	N

Table 3. Testing program for rainfall-induced deformation of slopes

Parameter \ Test ID	*PS-L*	*PS-H*	*SS-L*	*SS-H*
Soil type	sand	sand	silty sand	silty sand
Prototype rainfall intensity (mm/hr)	7.4	87.7	7.4	87.7
Relative intensity	0.21	2.44	1.71	20.3

Unfortunately, pore water pressure readings were not obtained in all tests; only test SS-H had reliable results at measurement points depicted in Figure 3. Figure 4 shows the PPT measurements during test SS-H. It can be seen that prior to the onset of rainfall, suction (negative pore pressure) developed within the model at all locations, which is due to desaturation during the gravity increase to 60g. Upon rainfall initiation, pore pressure increased slowly at all points, with the first increase near the crest of the slope, indicating the rainfall infiltration and development of the wetting front. The advancement of the wetting front in the soil then leads to the increase in pore pressure at the other locations in order of their depth. The failure starts 1.25 sec after the onset of rainfall (1.25 hr in prototype time). As the rainfall continues, pore pressure increases, leading to positive pore pressures within the soil. However, PPT7 (the shallowest PPT, near the crest of the slope) indicated suction for the whole period of rainfall, although the pore pressure approached a value of zero (nearly saturated) immediately before the rainfall was stopped.

In order to explain the differences between the results obtained for sand and silty sand, one may consider the effect of silt content on permeability and Darcy velocity. The conventional scaling law considering the macroscopic response of the soil under increased gravity deduces that the Darcy velocity (v_m) in the N-g model is N times larger than that in the prototype (Taylor, 1994), where the flow path is considered to be N times larger in the prototype. However, according to Take et al. (2004), the underlying mechanism for static liquefaction of soil can be explained by the collapse of saturated voids which leads to a local and abrupt increase of the pore pressure, which in turn reduces the effective stress and strength of the soil, and consequently slope failure. Askarinejad et al. (2015) analysed the grain scale phenomenon of voids collapse and concluded that, if the structure of soil in an N-g model and prototype were the same, the scaling factor of length at the grain scale is equal to one (i.e. $L_p/L_m=1$). Thus, the scaling law for pore pressure dissipation time in the model and the prototype can be written as follows

$$t_{dissipation,m} = L_m / v_m = L_p \left(1/Nv_m\right) = t_{dissipation,p} / N \qquad (1)$$

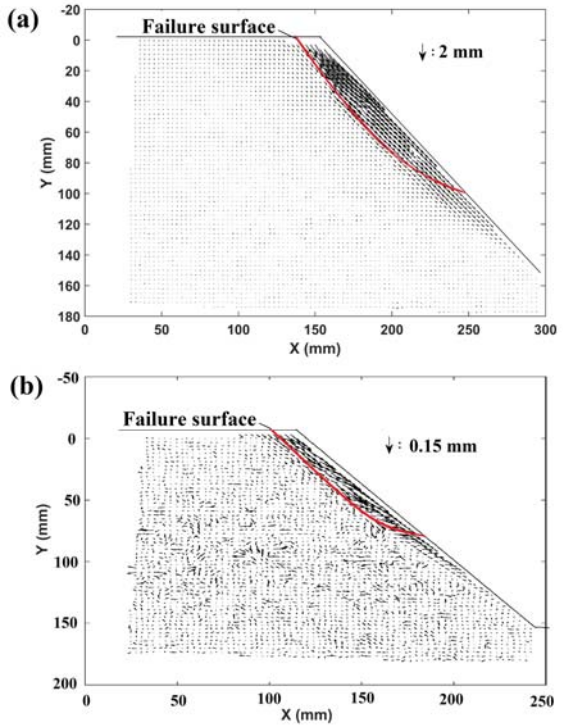

Figure 2. Rainfall-induced displacement vectors in slope models at failure initiation in (a) test SS-L at t= 1042 hr (b) test SS-H at t= 1.25 hr (t is prototype time)

In addition, Askarinejad et al. (2015) considered the collapse of the voids analogous to the free fall of particles, for which the time scaling law can be written as:

$$t_{impact,m} = \sqrt{2L_m / a_m} = \sqrt{2L_p / Na_p} = \sqrt{1/N}\; t_{impact,p} \qquad (2)$$

where a represents the acceleration, and L is the falling height. These relationships show that the pore water dissipation is $\sqrt{N}$ times faster than the collapse of the voids, which may also be related to the grain-scale movements required to initiate failure along a slip-plane.

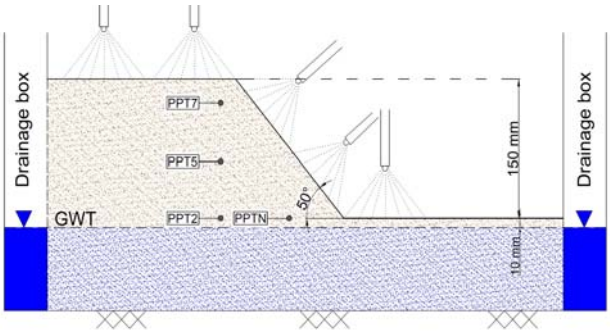

Figure 3. Pore water pressure measurement points for test SS-H

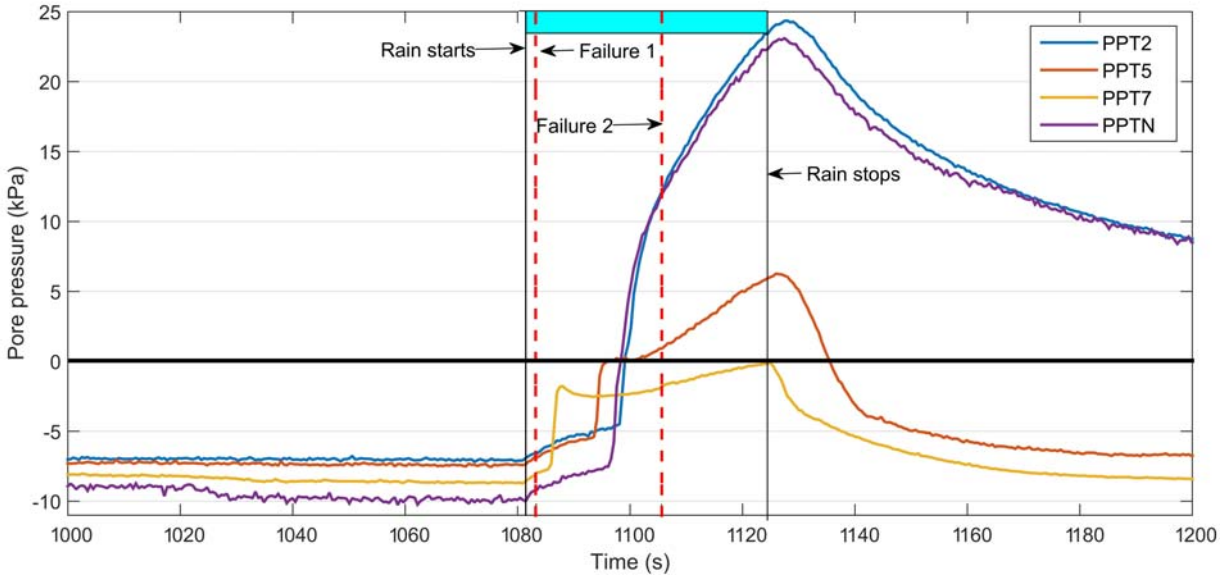

Figure 4. The evolution of pore water pressure at different points in test SS-H, in reference to the start and end of the rainfall event

These scaling factors may be used to explain the differences between the two types of soil used in this study. In case of sand, the pore water seepage is faster than the collapse of the voids and hence the time scale between the two coupled processes of dissipation and void collapse are incompatible. Thus, the pore pressure is dissipated before the void collapse occurs. In order to rectify this issue, Askarinejad et al. (2015) increased the viscosity of the pore fluid by a factor of $\sqrt{N}$. In this study, water is used as the pore fluid, but the use of silty sand provides models with a permeability ratio of 8.3 compared to the sandy models, nearly equal to $\sqrt{N}$=7.75. This suggests that adding 10% silt essentially reduces the permeability of the soil and is equivalent to the case where the fluid viscosity is increased by the same factor. In other words, if the viscosity of the fluid increases by a factor of 8.3 in case of sandy soil tests (PS-L and PS-H), failure is expected, similar to those observed in tests SS-L and SS-H. This may also explain why the test SS-L with relative intensity of 1.71 led to slope failure whereas test PS-H with a higher relative intensity (2.44) did not result in a failure. In test PS-H, the pore pressure dissipation phenomenon is 7.75 times faster than that of a free falling particle, and hence the pore pressure dissipates before the void collapse can happen. On the other hand, in test SS-L, pore pressure and void collapse have the same time scales which allow the test to properly simulate the prototype conditions. The presented interpretation and discussions, however, need further testing to validate the theoretical fundamentals discussed above, where pore pressure data are collected from a larger number of tests with enhanced spatial resolution.

4 CONCLUSIONS

Results of centrifuge models were presented in this paper to discuss how different soil slopes respond to rainfall. The sandy slope was stable under both low and high rainfall intensity, but the silty sand failed in both cases. The analysis of the results showed that silty sand in SS-L test failed even though its relative intensity was lower than that of the sandy slope PS-H. The different responses between the two soil types were attributed to the difference in time scales of void collapse and pore pressure dissipation. Further studies are required to give a better understanding of the impact of soil characteristics on slope instability mechanisms within the geotechnical centrifuge.

5 ACKNOWLEDGEMENTS

The authors would like to acknowledge the funding received from the People Programme (Marie-Curie Actions) of the European Union's Seventh Framework Programme FP7/2007-2013/ under REA grant agreement N° 289911, and European Commission's Research Fund for Coal and Steel (RFCS) under grant agreement N° RFCR-CT-2015-00001 (SLOPES project).

6 REFERENCES

Askarinejad, A., Beck, A., Springman, S.M., 2015. Scaling law of static liquefaction mechanism in geocentrifuge and corresponding hydromechanical characterization of an unsaturated silty sand having a viscous pore fluid. *Canadian Geotechnical Journal* 52, 708-720.

Germer, K., Braun, J., 2011. Effects of Saturation on Slope Stability: Laboratory Experiments Utilizing External Load. *Vadose Zone Journal* 10, 477-486.

Guzzetti, F., Peruccacci, S., Rossi, M., Stark, C.P., 2008. The rainfall intensity–duration control of shallow landslides and debris flows: an update. *Landslides* 5, 3-17.

Ling, H., Wu, M., Leshchinsky, D., Leshchinsky, B., 2009. Centrifuge Modeling of Slope Instability. *Journal of Geotechnical and Geoenvironmental Engineering* 135, 758-767.

Matziaris, V., Marshall, A.M., Yu, H.-S., 2015. Centrifuge Model Tests of Rainfall-Induced Landslides, in: Wu, W. (Ed.), Recent Advances in Modeling Landslides and Debris Flows. Springer International Publishing, Cham, pp. 73-83.

Take, W.A., Bolton, M.D., 2003. Tensiometer saturation and the reliable measurement of soil suction. *Géotechnique* 53, 159-172.

Take, W.A., Bolton, M.D., Wong, P.C.P., Yeung, F.J., 2004. Evaluation of landslide triggering mechanisms in modell fill slopes. *Landslides* 1, 173-184.

Taylor, R.N., 1994. Geotechnical centrifuge technology. CRC Press.

Tohari, A., Nishigaki, M., Komatsu, M., 2007. Laboratory Rainfall-Induced Slope Failure with Moisture Content Measurement. *Journal of Geotechnical and Geoenvironmental Engineering* 133, 575-587.

Zhang, L.L., Zhang, J., Zhang, L.M., Tang, W.H., 2011. Stability analysis of rainfall-induced slope failure: a review. *Proceedings of the Institution of Civil Engineers - Geotechnical Engineering* 164, 299-316.